on questions such as whether degeneration and dosage compensation usually evolve on a stepwise, gene-by-gene basis (*21*) or involve large blocks of chromosomal material (*13*). Secondary sex chromosomes, in which neo-X and neo-Y chromosomes have been created by centric fusions between old-established sex chromosomes and autosomes, are also a rich potential source of new facts (*27*).

REFERENCES AND NOTES

1. J. M. Smith, *The Evolution of Sex* (Cambridge Univ. Press, Cambridge, 1978).
2. J. J. Bull, *Evolution of Sex Determining Mechanisms* (Benjamin Cummings, Menlo Park, CA, 1983).
3. M. J. D. White, *Animal Cytology and Evolution* (Cambridge Univ. Press, Cambridge, 1973).
4. B. John, in *Heterochromatin: Molecular and Structural Aspects,* R. S. Verma, Ed. (Cambridge Univ. Press, Cambridge, 1988), pp. 1–147.
5. N. A. Ellis and P. N. Goodfellow, *Trends Genet.* **5**, 406 (1989).
6. A. Lohe and P. Roberts, in *Heterochromatin: Molecular and Structural Aspects,* R. S. Verma, Ed. (Cambridge Univ. Press, Cambridge, 1988), pp. 148–186.
7. E. M. Eicher, K. W. Hutchison, S. J. Phillips, P. K. Tucker, B. K. Lee, *Genetics* **122**, 181 (1989).
8. T. Dobzhansky, *ibid.* **20**, 366 (1935).
9. J. C. Lucchesi, *Science* **202**, 711 (1978); J. Hodgkin, *Nature (London)* **344**, 721 (1990).
10. M. Westergaard, *Adv. Genet.* **9**, 217 (1958).
11. H. J. Muller, *Genetics* **3**, 422 (1918).
12. R. A. Fisher, *Am. Nat.* **69**, 446 (1935).
13. B. Charlesworth, *Proc. Natl. Acad. Sci. U.S.A.* **75**, 5618 (1978).
14. C. D. Darlington, *Evolution of Genetic Systems* (Oliver & Boyd, Edinburgh, 1958).
15. C. R. Darwin, *The Different Forms of Flowers on Plants of the Same Species* (John Murray, London, 1877).
16. D. Charlesworth and B. Charlesworth, *Proc. R. Soc. London Ser. B.* **205**, 513 (1979); *Evolution* **41**, 948 (1987).
17. D. Charlesworth, in *Evolution: Essays in Honour of John Maynard Smith*, P. J. Greenwood, P. H. Harvey, M. Slatkin, Eds. (Cambridge Univ. Press, Cambridge, 1985), pp. 237–269.
18. R. A. Fisher, *Biol. Rev.* **6**, 345 (1931); W. R. Rice, *Evolution* **41**, 911 (1987).
19. J. A. Endler, in *Predator–Prey Relationships*, M. E. Feder and G. V. Lauder, Eds. (Univ. of Chicago Press, Chicago, 1986), pp. 109–134.
20. W. D. Hamilton, *Science* **156**, 477 (1967); M. Nei, *Am. Nat.* **104**, 311 (1970).
21. W. R. Rice, *Genetics* **116**, 161 (1987).
22. H. J. Muller, *Mutat. Res.* **1**, 2 (1964); J. Haigh, *Theor. Popul. Biol.* **14**, 251 (1978).
23. B. Charlesworth and C. H. Langley, *Annu. Rev. Genet.* **23**, 251 (1989).
24. _____, W. Stephan, *Genetics* **112**, 359 (1986); W. Stephan, *Mol. Biol. Evol.* **6**, 198 (1989).
25. D. G. Lloyd, *Plant Syst. Evol.* **131**, 71 (1979); B. B. Casper and E. L. Charnov, *J. Theor. Biol.* **96**, 143 (1982); D. Charlesworth, *ibid.* **139**, 327 (1989).
26. B. Charlesworth, in preparation.
27. E. Strobel, C. Pelling, N. Arnheim, *Proc. Natl. Acad. Sci. U.S.A.* **75**, 931 (1978); M. Steinemann, *Chromosoma* **89**, 59 (1982).

28. I thank D. Charlesworth, C. Langley, and W. Stephan for their collaborations on many of the ideas reviewed here; J. Bull for comments on the manuscript; and the National Science Foundation and the National Institutes of Health for supporting some of the research reviewed here.

Physics in Strong Magnetic Fields Near Neutron Stars

ALICE K. HARDING

Electromagnetic phenomena occurring in the strong magnetic fields of neutron stars are currently of great interest in high-energy astrophysics. Observations of rotation rate changes and cyclotron lines in pulsars and γ-ray bursts indicate that surface magnetic fields of neutron stars often exceed 10^{12} gauss. In fields this strong, where electrons behave much as if they were in bound atomic states, familiar processes undergo profound changes, and exotic processes become important. Strong magnetic fields affect the physics in several fundamental ways: Energies perpendicular to the field are quantized, transverse momentum is not conserved, and electron-positron spin is important. Neutron stars therefore provide a unique laboratory for the study of physics in extremely high fields that cannot be generated on Earth.

PHYSICAL CONDITIONS INFERRED TO EXIST IN ASTROPHYSICAL sources are often far outside the realm of conditions now achievable in laboratories on Earth. The highest magnetic fields in Earth-bound experiments, generated by implosive flux-compression (*1*), are in the tens of megagauss. Some white dwarf stars have fields that are about 10 times higher. The discovery of radio pulsars and then of x-ray binaries and γ-ray bursts revealed that neutron stars have fields that are a million times higher (10^{12} G), possibly the highest fields occurring in nature. In teragauss magnetic fields the cyclotron energy approaches the electron rest mass, and quantum effects become important. Many neutron stars emit radiation at x-ray and γ-ray energies, requiring acceleration of particles to at least tens of megaelectron volts. The combination of relativistic particle energies and quantizing magnetic fields requires a quantum electrodynamic (QED) description of the physical processes. By observing the radiation emitted by neutron stars, we can study the physical processes that are thought to occur only in these extremely high magnetic fields. This article reviews some of the theoretical work on the physics in strong magnetic fields as well as what observations of neutron stars can tell us about the behavior of radiative processes under these extreme conditions.

The author is an astrophysicist at the Laboratory for High Energy Astrophysics, National Aeronautics and Space Administration, Goddard Space Flight Center, Greenbelt, MD 20771.

Neutron Star Magnetic Fields

There are presently two ways to measure neutron star magnetic fields, and both independently indicate field strengths exceeding 10^{12} G. The first method involves monitoring neutron star rotation periods and determining their rate of change. The periods of radio pulsars are observed to increase with time. It is now widely accepted that these isolated neutron stars can be modeled as rotating magnetic dipoles emitting electromagnetic dipole radiation that creates a torque, causing them to spin down in a well-determined way. Because this torque is related to the star's magnetic dipole moment as well as to its moment of inertia I ($\sim 10^{45}$g $\cdot$ cm^2) and radius R_0 ($\sim 10^6$ cm), the surface magnetic field strength B_0 can be expressed in terms of the period derivative $\dot{P}$ as

$$B_0 \approx \left(\frac{3Ic^3P\dot{P}}{8\pi^2R_0^6}\right)^{1/2} = 3.2 \times 10^{19}\ \mathrm{G}\ (P\dot{P})^{1/2} \qquad (1)$$

where c is the speed of light.

Figure 1 shows the distribution of observed values of P and $\dot{P}$ of 308 radio pulsars and the range of surface magnetic fields as computed from Eq. 1. Although there is a range in inferred field strengths of nearly four decades, most pulsars have fields between 10^{11} and 10^{13} G, with a few even exceeding 10^{13} G. Magnetic fields also have been measured indirectly from the period derivatives of x-ray pulsars. These sources are neutron stars that radiate by accreting material from a binary companion. The accretion torques tend to spin up the neutron star, and the resulting $\dot{P}$ can be related to the magnetic field strength (*2*). Observed values of $\dot{P}$ for a number of x-ray pulsars also give magnetic fields around 10^{12} G.

The second method directly measures the magnetic field strength from the energies of cyclotron absorption lines in high-energy x-ray spectra of neutron stars. These line features appear as a result of resonant scattering or absorption of radiation by electrons at cyclotron harmonics, which should occur at roughly integral multiples of the cyclotron frequency. The cyclotron frequency ω_B is directly related to the magnetic field strength B as

$$\omega_B = \frac{eB}{mc} \simeq 12\ \mathrm{keV}\ B_{12} \qquad (2)$$

where e is the electron change, m is the electron rest mass, and $B_{12} \equiv B/10^{12}$ G.

Cyclotron lines were first observed in the spectra of x-ray pulsars, with the strongest feature observed being from the source Hercules X-1 (*3*). Because it is a single feature on the steeply falling upper end of the spectrum, the line can be interpreted as either emission or absorption at the first harmonic. In the case of absorption, the cyclotron energy is approximately 38 keV, giving a field strength of 3×10^{12} G; in the case of emission the cyclotron energy is approximately 50 keV, implying that $B = 4 \times 10^{12}$ G. If multiple features are observed, as they have been in several other x-ray pulsars and most recently in three γ-ray burst sources, then the cyclotron frequency can be determined precisely. Figure 2 shows the spectrum of a γ-ray burst with two cyclotron harmonics at 20 and 40 keV, implying a magnetic field of 1.7×10^{12} G.

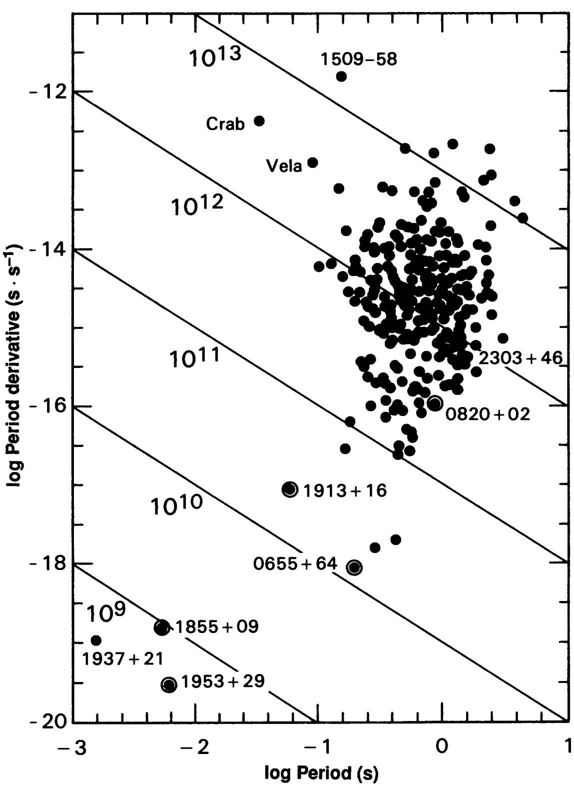

Fig. 1. Distribution of observed periods and period derivatives of 308 radio pulsars (*28*). The circled dots indicate binary pulsars. The superimposed diagonals are lines of constant surface magnetic field strength (in gauss).

QED Processes in Strong Magnetic Fields

The strong magnetic fields near neutron stars affect physical processes in several fundamental ways. First, momentum perpendicular to the field direction is quantized, so that electrons and positrons must occupy discrete Landau states with energy

$$E_n = mc^2[1 + (p/mc)^2 + 2nB']^{1/2} \qquad (3)$$

where $n = 0, 1, 2, \ldots$. In each state, particles may have a spin either up or down along the field direction except in the ground state $n = 0$, where only the spin-down state is allowed. The momentum component parallel to the field, p, is continuous, and $B' = B/B_{cr}$ is the magnetic field in units of the critical field ($B_{cr} \equiv m^2c^3/e\hbar = 4.414 \times 10^{13}$ G, where $\hbar$ is Planck's constant over 2π), in which the cyclotron energy equals the electron rest mass. Because $\hbar\omega_B = mc^2B'$, the Landau states are separated by the cyclotron energy in the nonrelativistic limit. The major manifestation of the discrete electron states is strong resonant behavior of the various cross sections.

Second, transverse momentum is not strictly conserved in interactions because the magnetic field can absorb or supply momentum (parallel momentum and total energy are strictly conserved). Thus a number of first-order processes are allowed that are forbidden in free space. Among these are cyclotron radiation and absorption, which are familiar as classical electromagnetic processes in weak fields, as well as one-photon pair production and annihilation, which become important only in strong fields approaching B_{cr}.

Third, in very strong fields processes depend on the spin of the electrons and positrons. One important effect is that transitions in which particles change spin (spin-flip transitions) are less probable than those in which the spin is unchanged.

In fields approaching the critical field strength, where the cyclotron energy is near the electron rest mass, an accurate description of the physics requires a fully relativistic treatment, that is, QED. This is true even when particle energies are nonrelativistic. Transition probabilities in QED can be derived from the square of the S-matrix element, in which the electron and positron wave functions are eigenfunctions of the Dirac equation in a static, homogeneous magnetic field and the photon is treated as a plane-wave perturbation. In processes such as bremsstrahlung and Coulomb scattering, potentials of the external fields are also treated as perturbations. This article will not go into details of the calculations but will concentrate on highlighting the important and unusual characteristics of a few radiative processes that are unique to strong fields. More detailed descriptions may be found in reviews by Harding (*4*) and Meszaros (*5*).

Cyclotron Emission

Cyclotron radiation and its inverse, cyclotron absorption, are first-order processes whose characteristics are familiar at low field strengths (*6*, *7*). In high fields approaching the critical field, the classical description breaks down in several ways, and a quantum description is required to compute accurately the radiative rates and photon spectrum, even for nonrelativistic electrons. In the quantum description of cyclotron radiation, electrons emit photons by spontaneously decaying from higher to lower Landau states. The classical picture of continuous emission by an electron executing smooth orbital motion is no longer valid. Furthermore, the classical distinction between cyclotron radiation, emission at low harmonics, and synchrotron radiation (in which the particle energy is relativistic and emission occurs at very high harmonics) becomes blurred in fields comparable to B_{cr}, where even emission at low harmonics is relativistic.

An example of the striking differences between classical and quantum descriptions of cyclotron radiation in strong magnetic fields is illustrated in Fig. 3. When $(B/B_{cr})[\gamma^2/(\gamma - 1)] > 1$, the energy of a photon at the classical value of the critical synchrotron radiation frequency, $\gamma^2\omega_B$, exceeds the electron kinetic energy $(\gamma - 1)mc^2$, where γ is the electron Lorentz factor. The classical emissivity therefore violates conservation of energy. The classical formula also overestimates the spectral emissivity when $\Gamma \equiv (B/B_{cr})\gamma > 0.1$. There is a consequent reduction of the electron energy loss rate from the classical formula, $\dot{\gamma} \propto \Gamma^2$, for large values of Γ (*8*). The overestimation of the emissivity by the classical formula is quite obvious for the parameters of Fig. 3, which may be typical of conditions in γ-ray bursts and radio pulsars. The approximation to the quantum formula for $n >> 1$, also shown in Fig. 3, incorporates a kinematic cutoff at $\omega = \gamma mc^2$ [a relativistic approximation to the true cutoff at $\omega = (\gamma - 1)mc^2$] and provides a much better estimate, except at the lowest harmonics. Because of electron recoil the harmonic energies are not simple multiples of the cyclotron frequency, as in the nonrelativistic case. The effect of spin-flip suppression in the transition rate is also apparent in Fig. 3. Because electrons with initial spin-up must undergo a spin-flip to decay to the ground state, their emissivity is less compared to that for electrons with initial spin-down.

Pair Production and Annihilation

Because an electron-positron pair has less momentum than a photon of the same energy, pair production by single photons is usually forbidden. In a strong magnetic field, which is able to absorb the extra momentum, electron-positron pairs can be produced by one photon as well as by two photons. The attenuation rate for conversion of a single photon into an electron-positron pair in the presence of an external magnetic field (also referred to as magnetic pair production) was first calculated in the early 1950s (*9, 10*), but because this process is not possibly observable in laboratory fields it did not receive much attention until the discovery of pulsars in the late 1960s. In both processes, the electron and positron can be produced only in the discrete Landau states that are kinematically available. When the photon energy is near threshold there may be only one or two of these states, and the cross sections will be resonant at each of the pair state thresholds.

Figure 4 shows the attenuation coefficient $\overline{R}$ for one-photon pair production as a function of photon energy for $\theta = 90°$, where θ is the angle of the photon direction with respect to the magnetic field. The threshold for producing a pair in the ground state is $2mc^2/\sin\theta$. Although this resonance structure is important very near threshold, the increasing density of resonances with photon energy allows the use of a more convenient asymptotic expression when the number of available pair states becomes large ($\sim 10^3$). In this limit, the probability of one-photon pair production rises exponentially with increasing photon energy and transverse field strength. A quick rule of thumb is that magnetic pair production will be important when $(E_\gamma/2mc^2)B' \sin\theta \geq 0.1$, where E_γ is the photon energy. Consequently, the quantum structure of near-threshold pair production becomes important when $B \gtrsim 4 \times 10^{12}$ G.

The strong angular dependence of the one-photon pair production threshold has important consequences for photon transport near neutron stars. For example, a 2-MeV photon propagating perpendicular to a strong field sees a pair production threshold at $2mc^2$ and will be absorbed, whereas the same photon propagating along the field would escape. Thus we might expect to observe high-energy cutoffs or turnovers in the spectra of neutron stars above 1 MeV as a result of pair production by the magnetic field. An even more exotic process that may attenuate photons in strong fields is photon splitting (*11*), which occurs as a result of the interaction of the photon virtual pairs with the magnetic field. When one member of a virtual electron-positron pair radiates, the photon splits into two photons of lower energy. The polarization of these pairs by the magnetic field also causes the vacuum to behave as an anisotropic medium, producing interesting propagation effects, such as birefringence, that might be observable in neutron star spectra (*12*).

The two-photon pair production cross section in a strong magnetic field also has resonances near threshold because of the discreteness of the pair states (*13*). The threshold depends on photon polarization direction with respect to the field, with the lowest threshold condition taking the form (*14*)

$$(E_1 \sin\theta_1 + E_2 \sin\theta_2)^2 + 2E_1E_2[1 - \cos(\theta_1 - \theta_2)] \geq 4m^2c^4 \tag{4}$$

where E_1 and E_2 refer to the energies of the photons and θ_1 and θ_2 are their angles with respect to the field. The second term is the same

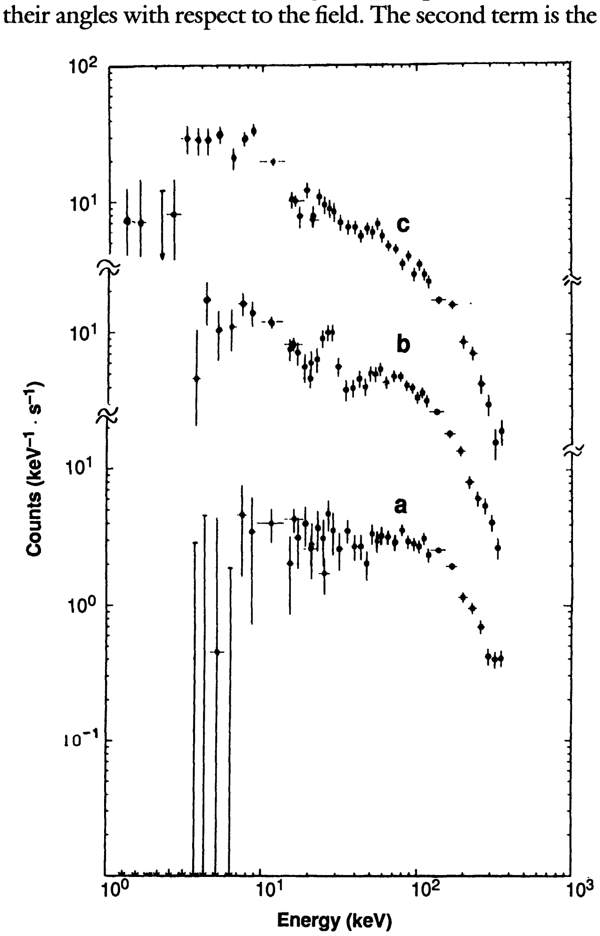

Fig. 2. Count spectra of the γ-ray burst GB880205 detected by the Ginga satellite at three successive times during the burst time history (*29*). Spectrum b shows absorption features near 20 and 40 keV.

Fig. 3. Cyclotron emission spectra [power per frequency interval, $I(\omega)$, in units of the cyclotron energy] from electrons at energy E. The histograms are Monte Carlo calculations of the quantum emissivity from electrons having initial spin-up (light histogram) or spin-down (bold histogram). The dashed curve is the classical emissivity, and the solid line is the asymptotic quantum emissivity (*30*).

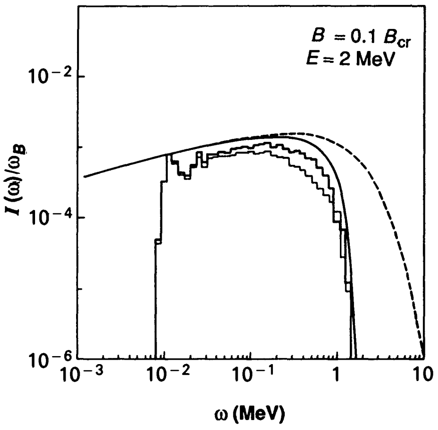

as the free-space threshold condition, and the first term appears as a result of nonconservation of perpendicular momentum. Thus it is possible for photons traveling parallel to each other ($\theta_1 = \theta_2 \neq 0^0$) to produce a pair, an event that is not permitted in free space.

In a strong magnetic field, electrons and positrons may annihilate into one or two photons through the inverse of the pair production processes discussed above. Because the synchrotron decay time in fields of about 10^{12} G ($\sim 10^{16}$ s) is much shorter than either collisional or annihilation time scales, pairs are expected to cool to the ground state before being annihilated. One-photon annihilation from the ground state results in a line at $2mc^2$ that is broadened asymmetrically by the parallel momenta of the pairs. Unlike the case in two-photon annihilation, Doppler broadening of the one-photon annihilation line results only in a blue shift because the photon must take all the kinetic energy of the pair in addition to the rest mass. The one-photon annihilation rate for pairs in the ground state increases exponentially with field strength but does not overtake the two-photon rate until around 10^{13} G (*14, 15*). Pairs annihilating from excited states would produce additional lines above 1 MeV, which at high energies blend together into a continuum (*16*).

Annihilation of electron-positron pairs into two photons produces a line at 511 keV, as in free space, but the relaxation of transverse momentum conservation in a high magnetic field causes an additional broadening of the line. For the case of annihilation of pairs at rest, the line is broadened by roughly $\Delta E \sim mc^2 B'/2$ for emission parallel to **B** and by

$$\Delta E \sim mc^2(B'/2)^{1/2} \sin\theta \qquad (\sin\theta > \sqrt{2B'}) \qquad (5)$$

for emission at angle θ to **B** (*14*). In fact, there is an increasing tendency in very high fields for one of the photons to be produced with almost all the pair's energy, so that two-photon annihilation behaves more like one-photon annihilation. Widths of observed two-photon annihilation lines in γ-ray burst spectra (*17*) could in principle put an upper limit on the magnetic field strength. The widths of even the narrowest emission features observed, however, are too large (probably as a result of thermal broadening) seriously to constrain the magnetic fields by the above relations.

Cyclotron Scattering and Absorption

Scattering and absorption of photons at cyclotron resonance energies are closely related processes, and both may result in spectral line features. Cyclotron absorption, the inverse of cyclotron emission, is a first-order process whereby photons at cyclotron-resonant frequencies induce upward transitions of electrons between Landau states. In the relativistic description, the resonant energies

$$\omega_n = mc^2[(1 + 2nB' \sin^2\theta)^{1/2} - 1]/\sin^2\theta \qquad (6)$$

are not exact multiples of the cyclotron energy $\omega_B = mc^2B'$ because the electron recoils on absorbing the photon. Cyclotron scattering is really resonant Compton scattering, a second-order process that is strongly resonant at the cyclotron harmonics. Because the second-order scattering description includes a virtual intermediate state, there are no kinematic constraints on the incident photon, as in absorption. Use of the first-order or second-order descriptions depends on whether the density is high enough that collisional deexcitation dominates over radiative deexcitation of electrons in excited Landau states. Even in the relatively dense accreted material that forms the hot emission region near the poles of x-ray pulsars, radiative deexcitation is expected to dominate as a result of the high magnetic field strength (*18*). Under these conditions, absorption of a cyclotron photon is always followed by the emission of another photon, so that resonant scattering is more important than resonant absorption near strongly magnetized neutron stars (*19*).

Figure 5 shows the relativistic cross section for scattering of an electron from the ground state to an arbitrary Landau state. The nonrelativistic magnetic scattering cross section (*20*) is resonant only at the fundamental cyclotron frequency, whereas the relativistic cross section is resonant at all higher harmonics. Excitation of electrons to excited Landau states through scattering is most important near the resonance energies. In fields $B << B_{cr}$, a photon with energy near ω_n will probably scatter an electron to state $n - 1$, resulting in a scattered photon at the cyclotron frequency with subsequent spontaneous emission of one or more cyclotron photons. This process is analogous to Raman scattering in atomic physics. The fact that resonant scattering is strongly dependent on harmonic number, field strength, and angle makes it an excellent diagnostic in the study of emission from neutron stars.

Cyclotron Resonant Scattering Models

A prime example of what we can learn about the behavior of radiative processes in strong magnetic fields from observations of neutron stars is the study of cyclotron line features in γ-ray bursts. These mysterious, transient sources emit bursts of emission almost exclusively in γ-rays, and although they are generally believed to be neutron stars the source of energy powering the bursts is not known [see (*4*) for review]. Single absorption features have been detected in

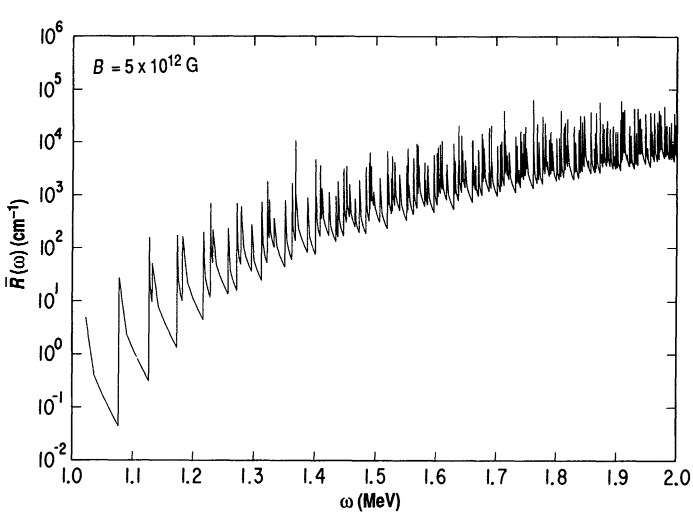

Fig. 4. Attenuation coefficient for one-photon pair production as a function of photon energy for propagation at 90° to the magnetic field (*31*).

about 20% of γ-ray burst spectra at energies between 30 and 60 keV. Their interpretation as cyclotron lines had for many years been controversial until the detection of double absorption features in the spectra of three γ-ray bursts by the Ginga satellite in 1988 (the spectrum of one of these bursts is shown in Fig. 2) laid to rest any doubt that the features were indeed cyclotron lines. More compelling is that detailed theoretical models (*21, 22*) have confirmed that cyclotron scattering physics can provide a completely consistent explanation for the line energies, widths, and depths.

The line at the first harmonic results from scattering of an electron in the ground state by a photon at the cyclotron frequency through a resonance at the first excited state. Because the incident and scattered photons are both at the cyclotron frequency, resonant photons are not destroyed, and the first harmonic is not a true absorption feature. An absorption-like feature can only form through multiple resonant scatterings in which the photon's energy gradually shifts out of the resonance as a result of the recoil of the electron. Because the cross section drops away from the resonance, there is a much lower chance of scattering back into the resonance, causing a net depletion of photons in the line core. The line at the second harmonic results from resonant scattering of photons with twice the cyclotron frequency. In most cases, however, the scattered photon appears at the first harmonic (leaving the electron in the first excited state) rather than at the second harmonic (leaving the electron in the ground state). Thus most second-harmonic photons leave the line core in a single scattering, approximating true absorption. An initially surprising feature of the observed lines, that the first and second harmonics are of similar strength even though the resonant scattering cross section decreases rapidly with harmonic number, can be explained naturally by this spawning of cyclotron photons through scattering events at higher harmonics, which partially fill in the first harmonic dip.

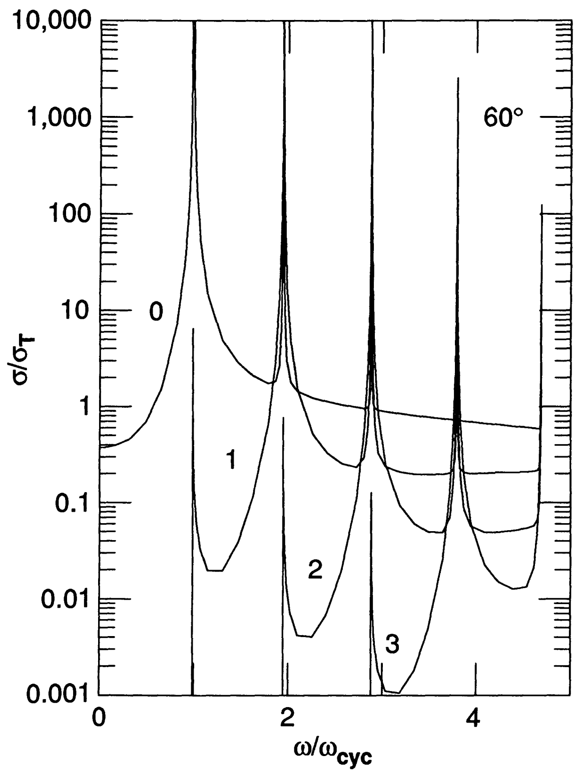

Fig. 5. Compton scattering cross section σ (in units of the Thomson cross section σ_T) at an incident angle of 60° as a function of incident photon frequency (in units of the cyclotron frequency) for electrons at rest in the ground state in a magnetic field of 1.7×10^{12} G. Labels refer to the final electron Landau state (*32*).

Fig. 6. Cyclotron line scattering profiles ϕ at different incident photon angles in a magnetic field of 1.7×10^{12} G. These profiles are the scattering cross section convolved with a one-dimensional thermal electron distribution at a temperature of 5 keV (*25*).

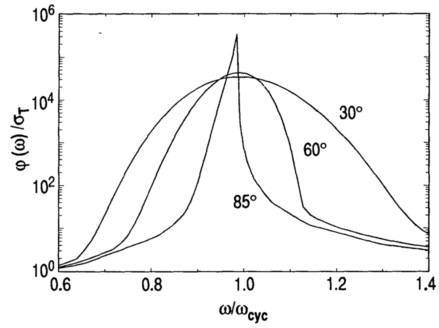

Another surprising feature of the observed lines is their narrow widths, which require a temperature of only about 5 keV, much cooler than that of the continuum (which is ~1 MeV). The low temperature can also be naturally explained with resonant scattering (*23*), which dominates the thermal balance of electrons in the scattering layer. The electrons will reach an equilibrium temperature, characterizing their parallel momentum distribution in the ground state, at which energy gains equal energy losses through scattering. The predicted equilibrium temperature is one quarter of the cyclotron frequency, which for a field strength of 1.7×10^{12} G is about 5 keV.

The assumption of a one-dimensional momentum distribution of scattering electrons in the ground state leads to extremely angle-dependent and asymmetric line profiles. The asymmetry results from the relativistic kinematics of one-dimensional Doppler broadening and is important in this case even when the electrons are nonrelativistic (*24, 25*). In the nonrelativistic limit, the width of line profiles due to Doppler broadening by a one-dimensional thermal electron distribution at temperature T is

$$\Delta\omega_D = \omega_n(2kT/mc^2)^{1/2} \cos\theta \qquad (7)$$

(where k is Boltzmann's constant), and the lines would be symmetric. Figure 6, however, shows that in a relativistic calculation of the scattering profile this is not the case. The relativistic correction is especially evident in the profile at angles near 90° to the field direction, where there would be almost no Doppler broadening in the nonrelativistic case. There is substantial transverse (second-order) Doppler broadening in the relativistic case, and it is exclusively a redshift.

Figure 7 shows the results of computer simulation of the cyclotron scattering process. In these codes, an assumed continuum spectrum is incident on a layer of constant electron density, parallel temperature, and magnetic field strength, and the resonant scattering of photons is computed as they propagate through the layer. The calculations show that the relative depths and shape of the harmonics are sensitive to viewing angle as well as to the optical depth of the layer. When the theoretical output spectrum at different angles is compared to data from one of the Ginga bursts, a magnetic field of 1.7×10^{12} G, an electron column depth (density × thickness) of 1.2×10^{21} electrons per square centimeter in the scattering layer, and an observation angle of 72° to the magnetic field provide the best fit to the data (*21*). At least in this particular burst, we are looking through a thin scattering layer and at a large angle to the field direction.

Future Possibilities

Anticipated observations at x-ray and γ-ray energies by planned space-based detectors have the potential to reveal much more about physics in strong magnetic fields. The four instruments on board the

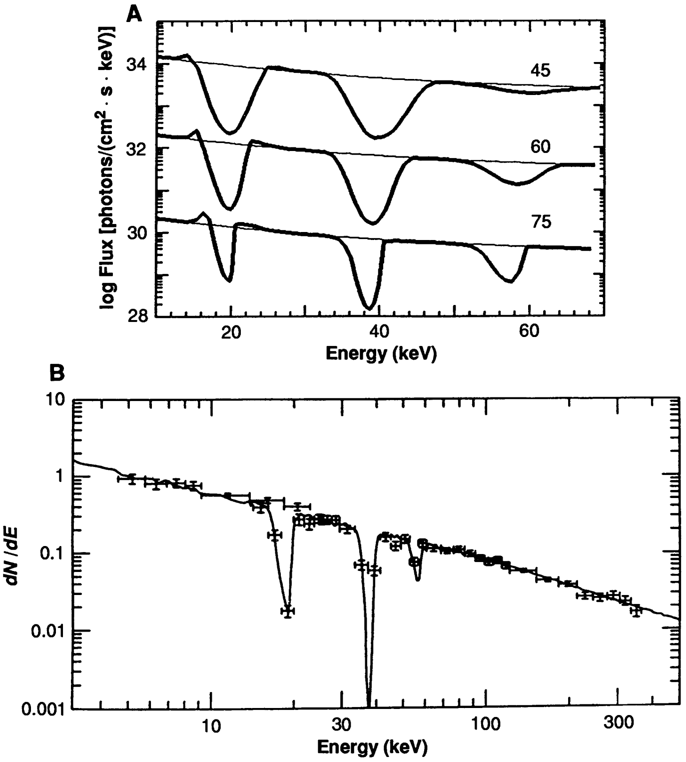

Fig. 7. (**A**) Model photon number spectra for cyclotron resonant scattering in a thin sheet with magnetic field $B = 1.7 \times 10^{12}$ G, Thomson optical depth 0.02, and one-dimensional electron temperature 5.2 keV at three different angles. [Adapted from (*22*) with permission of the author.] The light line is the incident photon spectrum. (**B**) Fit of cyclotron scattering model photon spectrum to data from Ginga burst GB880205 (*21*). Best-fit parameters are given in the text.

gamma-ray observatory (GRO), due to be launched in April 1991, will be capable of detecting radiation from neutron stars at energies between 10 keV and 10 GeV (*26*). Theoretically, high-energy cutoffs above 1 MeV in the spectra of γ-ray bursts and radio pulsars are expected from magnetic pair production. So far no definite cutoffs have been observed in spectra of these sources, but detectors on GRO will have the ability to search for pair-production turnovers at higher energies. The energies of any detected cutoffs will provide information about the origin and angular distribution of the emitted photons. Although there is evidence for two-photon pair annihilation lines in some γ-ray burst spectra, no evidence for a one-photon annihilation line has been seen. The burst and transient source experiment on GRO will have a much improved sensitivity around 1 MeV, where such lines would be expected. Detection of a one-photon annihilation line would indicate the presence of a magnetic field above 10^{13} G, and the ratio of one-photon to two-photon annihilation line flux would give a measure of the field strength. The improved energy resolution of other planned instruments (*27*) will make possible more detailed studies of cyclotron line shapes, from which we may be able to explore relativistic effects in resonant scattering as well as probe the emission regions of γ-ray burst sources. Future measurements of polarization at x-ray and γ-ray energies may even detect propagation effects due to the magnetic polarization of the vacuum.

REFERENCES AND NOTES

1. C. M. Fowler, W. B. Garn, R. S. Caird, *J. Appl. Phys.* **31**, 588 (1960); for a recent review see M. Miura *et al.*, *Physica B* **155**, 23 (1989).
2. P. Ghosh and F. K. Lamb, *Astrophys. J.* **234**, 296 (1979).
3. J. Trumper *et al.*, *ibid.* **219**, L105 (1978).
4. A. K. Harding, *Phys. Rep.*, in press.
5. P. Meszaros, *High Energy Radiation from Magnetized Neutron Stars* (Univ. of Chicago Press, Chicago, 1991).
6. G. Bekefi, *Radiation Processes in Plasmas* (Wiley, New York, 1966).
7. V. Canuto and J. Ventura, *Fundam. Cosmic Phys.* **2**, 203 (1977).
8. T. Erber, *Rev. Mod. Phys.* **38**, 626 (1966).
9. J. S. Toll, thesis, Princeton University (1952).
10. N. P. Klepikov, *Zh. Eksp. Teor. Fiz.* **26**, 19 (1954).
11. V. V. Usov and A. E. Shabad, *Sov. Astron. Lett.* **9**, 212 (1983); M. G. Baring, in *Proceedings of the Los Alamos Workshop on Gamma-Ray Bursts*, R. I. Epstein, E. E. Fenimore, C. Ho, Eds. (Cambridge Univ. Press, Cambridge, 1991).
12. G. G. Pavlov and Yu. N. Gnedin, *Sov. Sci. Rev. E Astrophys. Space Phys.* **3**, 197 (1984); P. Meszaros and J. Ventura, *Phys. Rev. D* **19**, 3565 (1979).
13. A. A. Kozlenkov and I. G. Mitrofanov, *Sov. Phys. J. Exp. Theor. Phys.* **64**, 1173 (1987).
14. J. K. Daugherty and R. W. Bussard, *Astrophys. J.* **238**, 296 (1980).
15. G. Wunner, *Phys. Rev. Lett.* **42**, 79 (1979).
16. A. K. Harding, *Astrophys. J.* **300**, 167 (1986).
17. E. P. Mazets *et al.*, *Nature* **290**, 378 (1981).
18. J. Ventura, W. Nagel, P. Meszaros, *Astrophys. J.* **233**, L125 (1979).
19. R. W. Bussard and F. K. Lamb, in *Gamma-Ray Transients and Related Astrophysical Phenomena*, R. E. Lingenfelter, H. S. Hudson, D. M. Worrall, Eds. (American Institute of Physics, New York, 1982), p. 189.
20. V. Canuto, J. Lodenquai, M. Ruderman, *Phys. Rev. D* **3**, 2303 (1971).
21. J. C. L. Wang *et al.*, *Phys. Rev. Lett.* **63**, 1550 (1989).
22. S. B. Alexander and P. Meszaros, *Astrophys. J.* **344**, L1 (1989).
23. D. Q. Lamb, J. C. L. Wang, I. M. Wasserman, *ibid.* **363**, 670 (1990).
24. D. Q. Lamb, J. C. L. Wang, T. J. Loredo, I. Wasserman, E. E. Fenimore, *Ann. N.Y. Acad. Sci.* **571**, 460 (1989).
25. A. K. Harding and J. K. Daugherty, *Astrophys. J.*, in press.
26. W. N. Johnson, Ed., *Proceedings of the GRO Science Workshop* (Naval Research Laboratory, Washington, DC, 1989).
27. R. I. Epstein, E. E. Fenimore, C. Ho, Eds., *Proceedings of the Los Alamos Workshop on Gamma-Ray Bursts* (Cambridge Univ. Press, Cambridge, 1991).
28. J. H. Taylor and D. R. Stinebring, *Annu. Rev. Astron. Astrophys.* **24**, 285 (1986).
29. T. Murakami *et al.*, *Nature* **335**, 234 (1988).
30. A. K. Harding and R. D. Preece, *Astrophys. J.* **319**, 939 (1987).
31. J. K. Daugherty and A. K. Harding, *ibid.* **273**, 761 (1983).
32. A. K. Harding and R. D. Preece, *ibid.* **338**, L21 (1989).
33. This article is based on an invited talk presented at the spring meeting of the American Physical Society in Washington, DC, April 1990.